Understanding the influence of boron oxide on the lithium polysulfides for improved lithium sulfur batteries: A DFT Study

C. Fwalo[1,2,*], B. D. Mahapane[1], R. E. Mapasha[1,3]

[1]*Department of Physics, University of Pretoria, Hatfield, Pretoria, 0028, South Africa*

[2] Department of Physics, Copperbelt University, Riverside, Kitwe, 10101, Zambia

[3]*National Institute for Theoretical and Computational Sciences, Matieland, Private Bag X1, South Africa*

*Email:fwalochewe99@gmail.com

Abstract. Ongoing research on lithium-sulfur battery (LiSB) aims to overcome setbacks caused by shuttle effects by exploring various cathode materials, with a particular focus on 2D materials such as boron oxide (BO) monolayer. The BO is gaining popularity due to its unique properties, such as ballistic electronic transport, mechanical strength, and large surface areas, making it a promising candidate as a cathode additive in LiSB. In this study, density functional theory (DFT) was used to investigate the interaction of lithium polysulfide (Li_2S_x where x = 1, 2, 4, 6, and 8, as well as S_8) with BO. The focus was on calculating the adsorption energy, charge density distribution, and metallic characteristics. The results showed Li_2S_x and S_8 strongly adsorbed on BO, with adsorption energy values between -0.34 and -1.64 eV, strong enough to prevent them from decomposing during the electrochemical processes. The charge density distributions support that there are strong electronic interactions in the systems, significant for the enhancement of battery cycle life. Furthermore, it was found that post-adsorption of non-conductive Li_2S and S_8 on BO, the metallic properties remained stable. Overall, results support BO as the best candidate for the cathode electrode in the next-generation LiSB.

1. Introduction

Enhancing energy storage systems to meet the growing demand has led to extensive investigations into battery technologies, particularly metal chalcogenide-based batteries like lithium-sulfur (LiSB) and sodium-sulfur batteries (NaSB) [1, 2], as well as lithium-selenium (LiSeB) and sodium-selenium batteries (NaSeB) [3]. Additionally, lithium and sodium-oxygen batteries have been explored [4, 5]. These systems exhibit significant potential due to their ultra-high theoretical specific capacities and energy densities [1, 6]. Among these technologies, LiSB has emerged as a promising candidate due to its low operational costs and environmentally friendly attributes [3]. During the charging process, the sulfur cathode reacts with lithium ions from the anode, yielding products such as Li_2S_x and S_8 [7].

Regardless the advantages over traditional lithium-ion batteries (LIB), LiSB faces several challenges that impede the development of a viable system. Key issues include sluggish movement of discharge products, poor electronic conductivity, and ineffective adsorption of discharge products by the cathode, which leads to their dissociation into the electrolyte during discharging [7]. These challenges are frequently linked to the materials selected for the cathodes. To address these challenges, significant research has focused on modifying cathode materials by tailoring their electronic properties and employing diverse fabrication techniques. Two-dimensional (2D) materials like

graphene [8] and silicene [9] are being explored for applications in metal-ion and air batteries [5], due to their favorable structural and electronic properties. Moreover, the BO monolayer has attracted considerable attention in recent years for its exceptional mechanical strength and intriguing anisotropies, making it a promising candidate for various electronic applications, including as a cathode additive in batteries.

Despite the extensive research on modifying the electronic properties of BO and its synthesis for various technological applications, there is limited information regarding its utilization in energy storage systems like LiSB. In this work, density functional theory (DFT) was employed to investigate the effects of Li_2S_x and S_8 on the electronic properties of BO and determine its use as a cathode additive in LiSB. The study focused on the electronic characteristics of BO following the adsorption of Li_2S and S_8. We meticulously optimized the crystal structure of BO and subsequently optimized the configurations of Li_2S_x and S_8 on it. Furthermore, we calculated the adsorption energies and associated charge density distributions for both the most stable and least stable discharge products, Li_2S and S_8, respectively. Finally, we assessed the electronic conductivity of BO post-adsorption.

2. Computational Methods

In this study, the DFT implemented in the quantum ESPRESSO code [12] was used for performing the calculations. The generalized gradient approximation (GGA) [13] within the functional of Perdew-Burke-Ernzerhoff (PBE) [14] was used to treat the exchange and correlation energies. The projector augmented wave (PAW) potential [15] was used to describe the core electrons. After conducting convergence tests, a kinetic energy cut-off of 748 eV was used. In addition, Monkhorst-Pack scheme [16] with a K-points sampling of 6 x 6 x 1 within the Brillouin zone [17] was used. The optimization of BO structure was achieved until all its atomic positions had converged within an energy difference of 10^{-5} eV and a Hellman-Feynman force convergence set to 10^{-6} eV/Å. To calculate the adsorption energy of Li_2S_x and S_8, the following equation was used:

$$E_{aver-ads} = \frac{E_{complex} - E_{substrate} - E_{free-species}}{n} \quad . \tag{1}$$

Here, $E_{(complex)}$ denotes the total energy of the BO adsorbed with polysulfides, $E_{(substrate)}$ is the total energy of the pristine BO, $E_{(free-species)}$ is the total energy of the free-species, and n is the total number of adsorbed Li_2S_x and S_8. Additionally, to calculate the charge density distributions in the systems of BO adsorbed with Li_2S_x and S_8, the following expression was used:

$$\Delta\rho = \rho_{(complex)} - \rho_{(substrate)} - \rho_{(free-adsorbate)} . \tag{2}$$

Here $\rho_{(complex)}$ represents the total charge density for the complex system (BO adsorbed with Li_2S_x and S_8), $\rho_{(substrate)}$ is the charge density for the isolated substrate from the complex system, $\rho_{(free-adsorbate)}$ charge density for the isolated Li_2S_x and S_8 from the complex system.

3. Results and Discussions

3.1 Adsorption of the Li_2S_x and S_8 on the BO

Comprehending materials' ability to adsorb species is very significant in the operation of the battery. This is because during the electrochemical process, discharge products are adsorbed by the electrode and are the ones that determine the specific capacity and energy density of the system. The stronger (higher) the adsorption energy, the lower the diffusion, the more efficient the battery becomes.

Therefore, we introduced the molecules as discharge products on the BO. The discharge products considered on the BO included the optimized molecules of Li_2S_x and S_8 as shown in Figure 1.

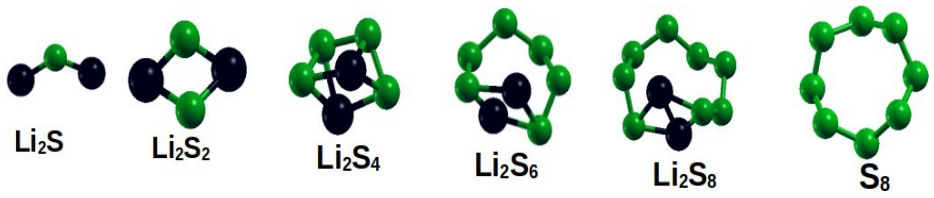

Figure 1: **Optimized molecules:**. Where the black and green balls denote Li and S atoms, respectively.

The molecules were tested at different adsorption sites on the BO based on its symmetry (Figure 2a), where it was determined that site H was the most stable; all the molecules diffused towards it. Subsequently, we optimized all the configurations at the identified site and calculated their corresponding adsorption energies as presented in Table 1.

Table 1: Calculated adsorption energies (eV) of the Li_2S_x and S_8 on BO.

System	Adsorption energy (eV)
Li_2S@BO	-1.64
Li_2S_2@BO	-1.02
Li_2S_4@BO	-1.03
Li_2S_6@BO	-0.77
Li_2S_8@BO	-0.58
S_8@BO	-0.34

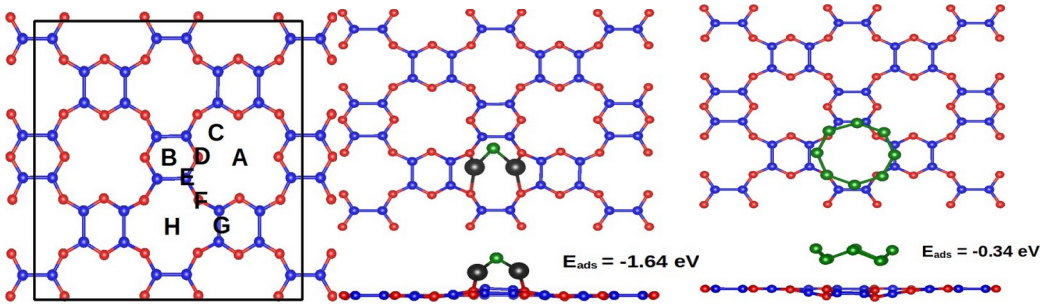

Figure 2: Optimized Configurations: (a) Possible adsorption sites and (b) Li_2S on BO, and (c) S_8 on BO. Where the black, blue, red, and green balls denote lithium (Li), carbon (C), oxygen (O), and sulfur (S) atoms, respectively.

The calculated adsorption energies for Li_2S_x and S_8 indicate that these species are strongly adsorbed on the BO surface. This strong adsorption suggests that they can effectively prevent dissociation into the electrolyte during the discharging process. Consequently, this finding highlights the potential of BO to mitigate the ongoing shuttle effects in LiSB.

3.2 Charge density distributions of the Li_2S and S_8 on BO

As the discharge products are adsorbed onto the surfaces of BO, electronic interactions within the systems are expected to occur. To investigate this, we calculated the charge density distributions, as illustrated in Figure 3. Firstly, we probed for the Li_2S on BO (Figure 3a), where it was observed that charge accumulated (yellow) towards the BO from the Li atoms, suggesting electronic interactions. And for the S_8 on BO (Figure 3b), a different trend was observed with charge accumulation towards the adsorbate, supported by the low adsorption energy obtained for S_8. Despite the charge being transferred towards the adsorbate, the BO is able to anchor the molecule; this is very significant as it is being prevented from dissociating into the electrolyte during the discharging process.

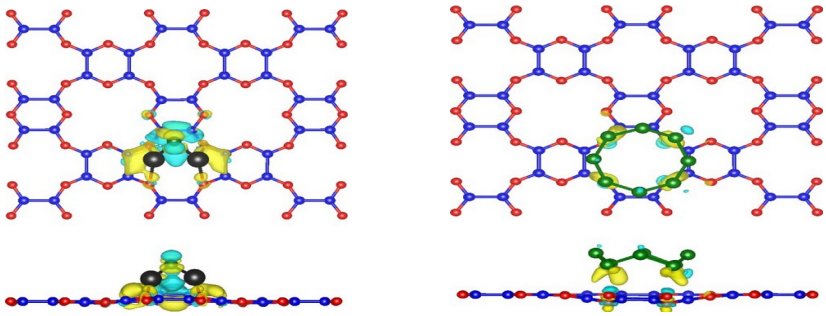

(a) (b)

Figure 3: **Charge density distributions: (a)** Li_2S on BO, and (b) S_8 on BO. Where charge accumulation and depletion are denoted by yellow and cyan colors, respectively.

3.3 Metallic properties of the BO adsorbed with Li_2S *and* S_8

The knowledge of the metallic properties of a material is crucial for its effectiveness as an electrode, as this allows for efficient electron transport during electrochemical processes. To thoroughly evaluate the metallic stability of BO, we performed detailed calculations of its electronic band structure, as illustrated in Figure 4a.

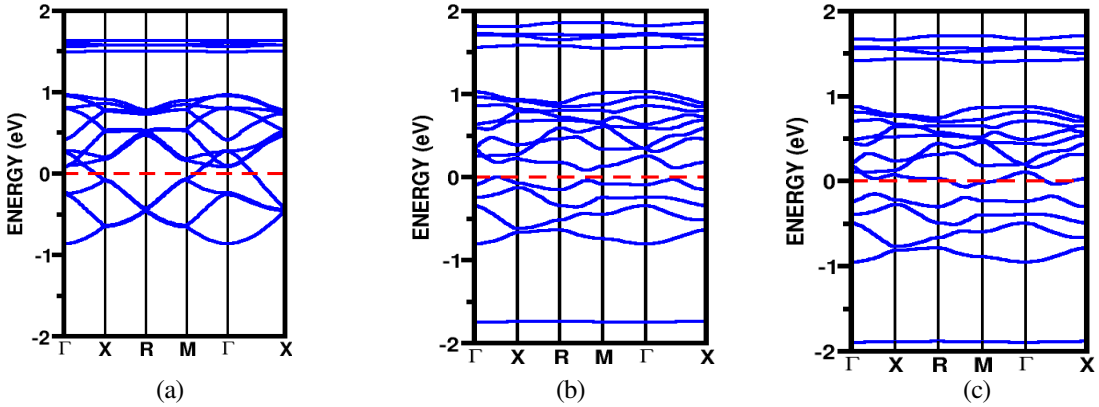

(a) (b) (c)

Figure 4: **Calculated bands structures:** (a) Pristine BO, (b) Li_2S on BO, and (c) S_8 on BO.

The findings indicated that pristine BO is metallic, characterized by the overlap of the valence and conduction bands, which facilitates the free flow of electrons, an essential feature for a viable electrode. Furthermore, we examined the alterations in the electronic structure following the

adsorption of non-conductive Li_2S and S_8, as depicted in Figures 4b and 4c, respectively. The results revealed that the adsorption of Li_2S impacted the electronic band structure of BO, leading to the formation of a band gap of 0.061 eV. Despite this gap, it was evident that the molecule was strongly adsorbed, as indicated in Table 1. The small gap created suggests that electrons can easily transition between the valence and conduction bands with minimal energy input.

In the case of S_8, it was observed that the valence and conduction bands still overlap despite the low adsorption energy value reported in Table 1. This observation is significant as it highlights the influence of BO on the adsorbate and promotes enhanced ion transport within the system. Consequently, the use of BO as a cathode additive could lead to an improved cycle life for LiSB applications.

4. Conclusion

In summary, DFT was used to investigate the influence of BO on the adsorbed Li_2S_x and S_8, assessing its potential application in LiSB. The findings revealed that Li_2S_x and S_8 are strongly adsorbed on BO, with adsorption energy values ranging from -0.34 to -1.64 eV, which is sufficient to prevent their decomposition during electrochemical processes. The charge density distributions indicate strong electronic interactions within the system, which are crucial for enhancing battery cycle life. Additionally, it was determined that BO exhibits metallic properties, characterized by overlapping bands, making it a significant candidate for use as an electrode. Interestingly, even after the adsorption of Li_2S and S_8, which are non-conductive, the electronic conductivity remained stable. Overall, results support BO as an electrode material for next-generation LiSB.

Conflicts of interests

There is no conflict of interest declared by the authors.

Acknowledgments

The University of Pretoria, Department of Innovation and Research, is gratefully acknowledged for its financial support. Additionally, the Center for High-Performance Computing (CHPC) in Cape Town, is recognized for providing exceptional computational resources. R.E.M. acknowledges the National Institute for Theoretical and Computational Sciences for its funding.

References

[1] L. Zhang, P. Liang, H.-b. Shu, X.-l. Man, F. Li, J. Huang, Q.-m. Dong, and D.-l. Chao, "Borophene as efficient sulfur hosts for lithium–sulfur batteries: suppressing shuttle effect and improving conductivity," *The Journal of Physical Chemistry C*, vol. 121, no. 29, pp. 15549–15555, 2017.

[2] S. Grixti, S. Mukherjee, and C. V. Singh, "Two-dimensional boron as an impressive lithium-sulphur battery cathode material," *Energy Storage Materials*, vol. 13, pp. 80–87, 2018.

[3] S. S. Deshpande, M. D. Deshpande, K. Alhameedi, R. Ahuja, and T. Hussain, "Carbon nitride monolayers as efficient immobilizers toward lithium selenides: potential applications in lithium–selenium batteries," *ACS Applied Energy Materials*, vol. 4, no. 4, pp. 3891–3904, 2021.

[4] C. Fwalo, A. Kochaev, and R. Mapasha, "Investigating electrocatalytic properties of β12-borophene as a cathode material for an efficient lithium-oxygen battery: a first-principles study," *Applied Nanoscience*, pp. 1–16, 2024.

[5] C. Xia, C. Kwok, and L. Nazar, "A high-energy-density lithium-oxygen battery based on a reversible four-electron conversion to lithium oxide," *Science*, vol. 361, no. 6404, pp. 777–781, 2018.

[6] Q. Li, H. Liu, Z. Yao, J. Cheng, T. Li, Y. Li, C. Wolverton, J. Wu, and V. P. Dravid, "Electrochemistry of selenium with sodium and lithium: kinetics and reaction mechanism," *ACS nano*, vol. 10, no. 9, pp. 8788–8795, 2016.

[7] F. Chen, C. Gao, H. Li, J. Hou, and D. Jiang, "FeS monolayer as a potential anchoring material for lithium-sulfur batteries: A theoretical study," *Surface Science*, vol. 707, p. 121818, 2021.

[8] A. H. Castro Neto, F. Guinea, N. M. Peres, K. S. Novoselov, and A. K. Geim, "The electronic properties

of graphene," *Reviews of Modern Physics*, vol. 81, no. 1, pp. 109–162, 2009.

[9] D. Jose and A. Datta, "Structures and chemical properties of silicene: unlike graphene," *Accounts of Chemical Research*, vol. 47, no. 2, pp. 593–602, 2014.

[10] P. Giannozzi, O. Andreussi, T. Brumme, O. Bunau, M. B. Nardelli, M. Calandra, R. Car, C. Cavazzoni, D. Ceresoli, M. Cococcioni, *et al.*, "Advanced capabilities for materials modelling with quantum espresso," *Journal of Physics: Condensed Matter*, vol. 29, no. 46, p. 465901, 2017.

[11] S. Grimme, "Semiempirical gga-type density functional constructed with a long-range dispersion correction," *Journal of Computational Chemistry*, vol. 27, no. 15, pp. 1787–1799, 2006.

[12] J. P. Perdew, K. Burke, and M. Ernzerhof, "Perdew, burke, and ernzerhof reply," *Physical Review Letters*, vol. 80, no. 4, p. 891, 1998.

[13] P. E. Blöchl, "Projector augmented-wave method," *Physical review B*, vol. 50, no. 24, p. 17953, 1994.

[14] H. J. Monkhorst and J. D. Pack, "Special points for brillouin-zone integrations," *Physical Review B*, vol. 13, no. 12, p. 5188, 1976.

[15] D. J. Chadi, "Special points for brillouin-zone integrations," *Physical Review B*, vol. 16, no. 4, p. 1746, 1977.